

# Creep mechanism of highly purified V-4Cr-4Ti alloys during thermal creep in a vacuum

メタデータ	<p>言語: English</p> <p>出版者:</p> <p>公開日: 2008-12-02</p> <p>キーワード (Ja):</p> <p>キーワード (En):</p> <p>作成者: FUKUMOTO, Ken-ichi, NAGASAKA, Takuya, MUROGA, Takeo, NITA, Nobuyasu, MATSUI, Hideki</p> <p>メールアドレス:</p> <p>所属:</p>
URL	<a href="http://hdl.handle.net/10098/1791">http://hdl.handle.net/10098/1791</a>

# **Creep mechanism of highly purified V-4Cr-4Ti alloys during thermal creep in a vacuum**

Ken-ichi Fukumoto<sup>1</sup>, Takuya Nagasaka<sup>2</sup>, Takeo Muroga<sup>2</sup>, Nobuyasu Nita<sup>3</sup>, Hideki Matsui<sup>3</sup>

<sup>1</sup>*Graduate School of Nuclear Power and Energy Safety Engineering: University of Fukui, Fukui 910-8507, Japan*

<sup>2</sup>*National Institute for Fusion Science, Toki, Gifu 509-5292, Japan*

<sup>3</sup>*Institute for Materials Research : Tohoku University, Sendai 980-8577, Japan*

## **Corresponding Author**

**Ken-ichi FUKUMOTO**

**Bunkyo 2-1-1, Fukui, 910-8507 Japan**

**TEL & FAX : +81-776-27-9712**

**e-mail : fukumoto@mech.fukui-u.ac.jp**

Keywords Code,

C1100 : Creep and stress relaxation

I0100 : Impurities

M0500 : Microstructure and Texture (excludes by Irradiation)

V0100 : Vanadium, vanadium alloys and compounds

# **Creep mechanism of highly purified V-4Cr-4Ti alloys during thermal creep in a vacuum**

Ken-ichi Fukumoto<sup>1</sup>, Takuya Nagasaka<sup>2</sup>, Takeo Muroga<sup>2</sup>, Nobuyasu Nita<sup>3</sup>,  
Hideki Matsui<sup>3</sup>

<sup>1</sup>Graduate School of Nuclear Power and Energy Safety Engineering: University  
of Fukui, Fukui 910-8507, Japan

<sup>2</sup>National Institute for Fusion Science, Toki, Gifu 509-5292, Japan

<sup>3</sup>Institute for Materials Research : Tohoku University, Sendai 980-8577, Japan

## **Abstract**

Pressurized thermal creep tubes of highly purified V-4Cr-4Ti, the NIFS-Heat2 alloy have been examined following testing in the range 700 to 850°C. It was found that the creep stress exponent of the NIFS-Heat2 alloy is about 5 and that the characteristic creep mechanism was the dislocation creep usually observed in pure metals. The apparent activation energy of creep deformation is about 210kJ/mol in the temperature range 700 to 850°C. Creep deformation was considered to be controlled by climb-controlled dislocation glide at 850°C, where sub-grain boundary structure predominates and consists of dislocation dipole structures and pile-ups of dislocations.

## **Introduction**

Vanadium alloys are candidate materials for fusion reactor blanket structural applications because of their potentially high operation temperatures. However the knowledge about the creep properties of vanadium alloys at fusion-relevant temperatures is limited and there are uncertainties that may have influenced the results such as the interstitial impurity content of specimens. In order to measure irradiation creep, several tests have been done using pressurized creep tubes (PCTs) [1-3]. Recently, high-purity V-4Cr-4Ti ingots (NIFS-HEAT-1 and 2) were provided by the National Institute for Fusion Science (NIFS), Japan [4-6]. In order to perform creep tests on highly purified V-4Cr-4Ti alloys, a manufacturing process for pressurized creep tubes has been established with the aim of avoiding contamination by interstitial impurities during the process [6,7].

The objective of this study is to investigate the thermal creep properties and microstructural changes of a highly purified V-4Cr-4Ti alloy, the NIFS-HEAT2, by using PCTs, as a preliminary study to enable future in-pile creep tests.

## **Experimental Procedures**

The V-4Cr-4Ti alloy used in this study was produced by NIFS and Taiyo Koko Co. and is designated NIFS-HEAT2 [5]. The detailed fabrication processes for tubing and for PCTs have been reported [6,7]. Table 1 shows the creep test conditions for PCTs. The PCTs wrapped with Ta and Zr foils were encapsulated in a quartz tube in a vacuum of  $< \sim 5 \times 10^{-3}$  Pa. In order to remove gas impurities from the quartz tube, about 100 cm<sup>2</sup> of Zr foil were included as a getter. Thermal creep tests were performed by placing the sealed quartz tubes in a muffle furnace. Dimensional changes of PCTs were measured with a precision laser profilometer manufactured by KEYENCE, LM-7030MT. Diameters were determined to an accuracy of  $\pm 1 \mu\text{m}$ . When the creep strain exceeded 20%, the creep test was terminated. Transmission electron microscopy (TEM) observations were performed on pieces cut from selected PCTs. The detailed fabrication procedure for TEM specimens from PCTs has been reported [2]. TEM observations were performed using a JEOL-2000FX at the Univ. of Fukui. Chemical analyses for oxygen and nitrogen were performed on two of the 850°C PCT specimens using the rest of the specimens.

## Results

## Creep strain measurement

Fig. 1 shows the time dependence of the effective mid-wall creep strain for 700°C, 750°C, 800°C and 850°C test temperatures. In fig.1, primary creep can not be observed as the duration of primary creep is expected to be short [8, 9].

Fig.2 shows an Arrhenius plot of creep strain rate obtained from data in Fig.1. Creep strain rates were determined by using data for effective strains less than about 1% to exclude any ternary creep data, even though the remaining number of data are few. From Fig.2, the activation energy for creep of V-4Cr-4Ti was estimated for effective stress levels of approximately 100 and 150MPa. Activation energies ranging from 197 to 227kJ/mol were obtained, with an average value of 210kJ/mol. The activation energies do not vary inversely with stress as has been observed for pure vanadium [8, 10]. These values are similar to those obtained for the NIFS-Heat in uniaxial creep tests about 180 to 210kJ/mol in the 750 - 800°C temperature range [9]. However, these values are somewhat smaller than the activation energy for self diffusion in pure vanadium, which is about 270kJ/mol in the 700-800°C temperature range [8, 11].

The stress dependence of creep strain rate was also deduced from Fig.1. The data in Fig.1 were fitted with the equation  $d\varepsilon/dt=A\sigma^n$ , where A is a constant,

n the creep stress exponent,  $\dot{\epsilon}$  the effective creep strain rate and  $\sigma$  is the effective stress. The stress exponent was found to be 4.9 for 800°C creep data. It has been reported that the strain exponents, n, for pure V and V-Ti alloys [10,12,13] are greater than 5 for creep test conditions similar to those used in this work, indicating that the creep mechanism is climb-assisted glide of dislocations.

The average oxygen and nitrogen levels have been measured to be 330 and 110wppm after 51h, and 520 and 140wppm after 118h for the 850°C PCT specimens. On the other hand, the oxygen content and the nitrogen content were 270wppm and 110wppm after 660h for the 750°C PCT specimens, respectively. These levels may be compared to the as-received values of 370wppmO and 100wppmN. It is indicated that impurity pick up does not occur in creep tests with a quartz tube due to careful sealing treatment. However, there is a possibility that residual gas impurity unexpectedly remained in the quartz tube and was absorbed by some specimens during vacuum encapsulation

### **Microstructural analysis**

The two specimens tested at 850°C were selected for TEM observation and for

chemical analyses in order to identify the operating creep mechanism. TEM micrographs of the NIFS-Heat2 alloy tested at 850°C are presented in Fig. 3. Moderately high dislocation densities can be seen in the 100MPa specimen, where the dislocations tend to be confined to sub-grain boundaries like cell structures and to lie in randomly arrays inside the sub-grains. On the other hand, dislocation cell structures are fully developed in a uniform array at regular intervals of about 0.8µm in the 150MPa specimen. Precipitates of Ti(OCN) are located in non-uniform distributions in grains and/or at grain boundaries. The precipitate particles were present prior to testing and did not change significantly as a result of creep testing; they are similar in size to those reported by Heo [14]. In order to identify the dislocation Burgers vectors, the  $\mathbf{g} \cdot \mathbf{b} = 0$  technique was applied. Such an analysis revealed that most of the free dislocations not associated with sub-grain boundaries in the 100MPa specimen are of the  $a/2\langle 111 \rangle$  type. Fig.4 shows TEM images of a dislocation array in the specimen tested at 850°C at a stress of 150MPa. The straight dislocations running from upper left to lower right consist of dislocations with two types of Burgers vector,  $[111]$  and  $[-111]$ . Orientation trace analysis show they are edge dislocations. Therefore, this dislocation array consists of edge dipoles made of different types

of dislocations. Other examples were found showing that the sub-grain boundaries were comprised mainly of edge dislocations

## **Discussion**

Both uniaxial [9, 15] and biaxial [8, 16] creep tests were performed in vacuum with different starting concentrations of interstitial O in recent studies. A review of thermal creep of V-Cr-Ti alloys by Kurtz [16], found the activation energy for creep between 700 and 800°C to be about 300kJ/mol, which is similar to the activation energy for self-diffusion in pure V. This suggests that in this regime of temperature and stress the predominant creep mechanism is climb-assisted dislocation motion. The apparent activation energy in the present study is 210kJ/mol for stresses between 100 and 150MPa. These values are lower than the activation energy found for the US-Heat #832665 of V-4Cr-4Ti, 299kJ/mol [8], and higher than the values found for V-2.8Ti, 125kJ/mol [12,17]. It has been reported that the strong scavenging effect of titanium and low oxygen solubility in V-3Ti correspond to the lowest activation energy for creep in V-Ti alloys [11]. This result indicated that the oxygen content may be significantly lower in V-3Ti than in any other V-Ti alloy and that the reduction of matrix impurity contents

may lead to a lower amount of activation energy. The reduction in oxygen and interstitial impurity content, may explain why the activation energies for NIFS-Heat alloys are lower than the energy for other V-4Cr-4Ti alloys containing above 1000wppm of O, C, N. It suggests that the reduction of impurity content lowers the potential barrier for vacancy diffusion and impurities in V-Cr-Ti alloys act as trapping site for vacancies, leading to the formation of Ti solute – impurity – vacancy complexes. It is also possible these complexes are obstacles to climb-assisted vacancy diffusion to dislocation cores in these creep conditions.

The power law dependence of the secondary creep rate on stress with  $n=4.9$ , in this study is in good agreement with the value of stress exponent of  $n \sim 4$  reported in a review of thermal creep for V-4Cr-4Ti by Kurtz [16]. This result also suggests that the operating creep mechanism is climb-assisted dislocation motion and this idea is supported by the microstructural analysis. The cell structure formation occurring during thermal creep also indicates that the creep mechanism is of pure metal type and that dislocation core diffusion plays an important role as the rate controlling process for creep deformation. The cell structure is made of arrays of edge dislocation dipoles formed during thermal creep and did not result from post-creep deformation. The other dislocation

arrays made of dislocations with one type of Burgers vector also appears to be formed during thermal creep. Both types of dislocation arrays formed in the same grain without free dislocations between cell walls indicating no post-creep deformation. The dependence of the microstructure on stress also suggests that at high stresses glide-controlled creep behavior predominates over the climb-controlled creep such that free dislocations in a sub-grain are absorbed in the sub-grain walls. The increase in density of free dislocations between sub-grain boundaries at lower stress levels indicates that climb controlled creep dominates and dislocations then distribute randomly. With increasing density of free dislocations, the creep stress exponent gradually decreases to a value of about 3, indicating a solid-solute creep behavior [18]. Since the target of this study was to explore creep deformation under moderately high stress level, the data are not sufficient to establish the creep mechanism diagram for V-4Cr-4Ti. Further work at lower stresses and elevated temperatures are needed to determine the thermal creep mechanisms as a baseline for future irradiation creep measurements.

## **Summary**

In order to investigate the thermal creep properties and microstructural changes of the highly purified NIFS-HEAT2 V-4Cr-4Ti, thermal creep tests were performed in the range 700 to 850°C using PCTs. The creep stress exponent for the NIFS-Heat2 alloy was about 5 which is characteristic of dislocation-glide creep observed in pure metals. The apparent creep activation energy of creep deformation was about 210kJ/mol in the temperature range 750 to 800°C. Microstructural analysis showed dislocation cell structures developed at 850°C under with the highest applied stress. This also suggests that climb-assisted glide of dislocations is the rate-limiting creep process at 850°C.

### **Acknowledgements**

This work was supported by NIFS Budget Code, NIFS04KFRF010.

## References

- [1] : H. Tsai, H. Matsui, M. C. Billone, R. V. Strain and D. L. Smith, J. Nucl. Mater. 258-263 (1998) 1471.
- [2] : K. Fukumoto, S. Takahashi, R. J. Kurtz, D. L. Smith and H. Matsui, J. Nucl. Mater. 341 (2005) 83.
- [3] : J.M. Vitek, D.N. Braski, J.A. Horak, J. Nucl. Mater. 141–143 (1986) 982.
- [4] : T. Muroga, T. Nagasaka, A. Iiyoshi, A. Kawabata, S. Sakurai, M. Sakata, J. Nucl. Mater. 283–287 (2000) 711.
- [5] : T. Muroga, T. Nagasaka, K. Abe, V.M. Chernov, H. Matsui, D.L. Smith, Z.-Y. Xu, S.J. Zinkle, J. Nucl. Mater. 307–311 (2002) 547.
- [6] : T. Nagasaka, T. Muroga, T. Iikubo, Fusion Sci. Tech. 44 (2003) 465.
- [7] : K. Fukumoto, H. Matsui, M. Narui, T. Nagasaka, T. Muroga, J. Nucl. Mater. 335 (2004) 103
- [8] : R. J. Kurtz and M. L. Hamilton, J. Nucl. Mater. 283-287 (2000) 628
- [9] : K. Fukumoto, T. Yamamoto, S. Nakao, S. Takahashi and H. Matsui., J. Nucl. Mater. 307-311 (2002) 610
- [10] : K.R. Wheeler, E.R. Gilbert, F.L. Yaggee, S.A. Duran, Acta Metall. 19

(1971) 21.

[11]: D.L. Harrod, R.E. Gold, Int. Met. Rev. 4 (1980) 163.

[12]: H. Boehm, et al., J.Less-Common Met. 12(1967) 280

[13]: T. Kainuma, N. Iwao, T. Suzuki and R. Watanabe, J.Less-Common Met.

86 (1982) 263

[14]: N. J. Heo, T. Nagasaka and T. Muroga, J. Nucl. Mater. 325 (2004) 53

[15]: K. Natesan, W.K. Soppet, A. Purohit, J. Nucl. Mater. 307–311 (2002)

585.

[16]: R.J. Kurtz, K. Abe, V.M. Chernov, D.T. Hoelzer, H. Matsui, T. Muroga, G.

R. Odette, J. Nucl. Mater. 329–333 (2004) 47

[17]: H. Boehm et al., Z.Metallkdet. 59 (1968) 715

[18]: J. Cadek, “Creep in metallic materials”, (Elsevier, 1988) p.115

### Figure captions

Fig.1. : Time dependence of the effective mid-wall creep strain of a highly purified V-4Cr-4Ti, the NIFS-Heat2 alloy for the 700, 750, 800 and 850°C test temperatures.

Fig.2. : Arrhenius plot of creep strain rate of a highly purified V-4Cr-4Ti, the NIFS-Heat2 alloy. Stress levels are 200, 150 and 90-110MPa.

Fig.3. : Examples of TEM images of a highly purified V-4Cr-4Ti, the NIFS-Heat2 alloy, tested at 850°C under creep stresses of 100MPa and 150MPa. Arrows indicate the directions related to the pressurized creep tube geometry; [L] indicates a longitudinal direction along the tube and [H] a hoop direction.

Fig.4. : Examples of TEM images of dislocation structures in the V-4Cr-4Ti alloy tested at 850°C with a stress of 150MPa. (A)  $(1\bar{1}0)$  diffraction vector, (B)  $(\bar{1}21)$  diffraction vector, (C)  $(121)$  diffraction vector, and (D) a characterization map for Burgers vector of dislocations. The arrow inserted in each photo shows the direction of the g-reflection.

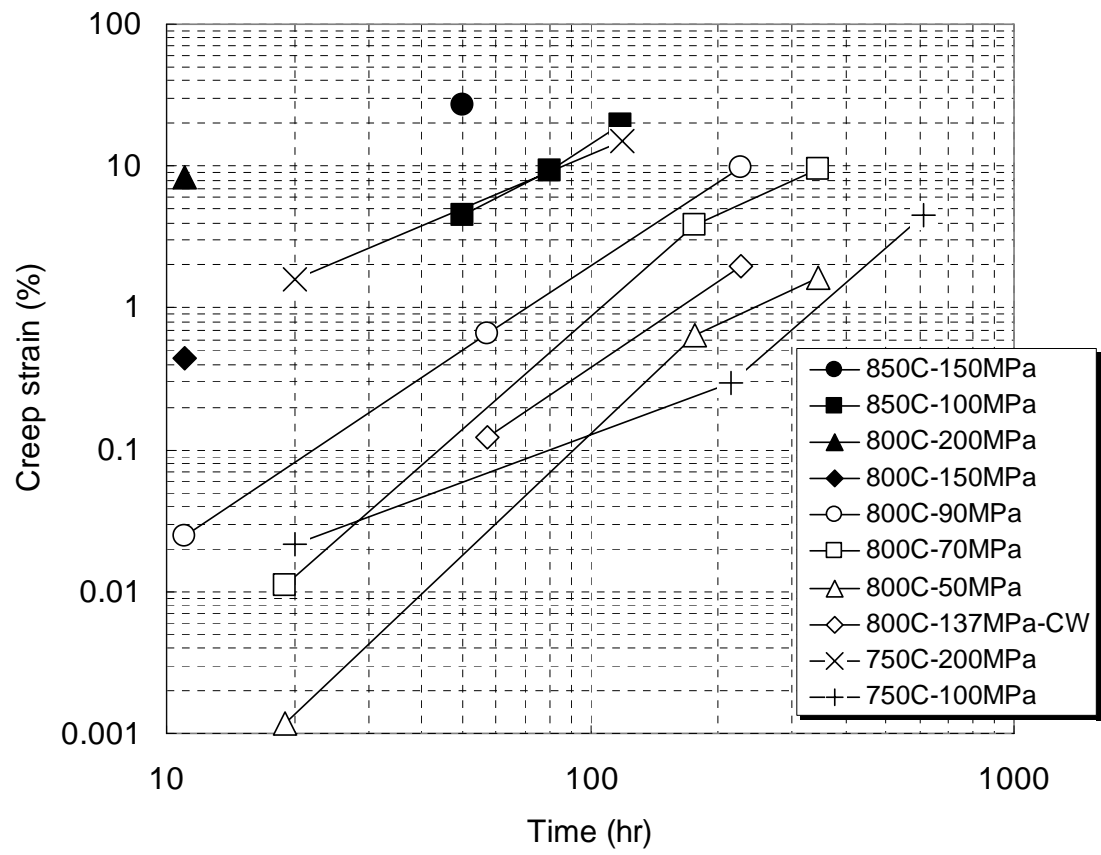


Fig.1 one column

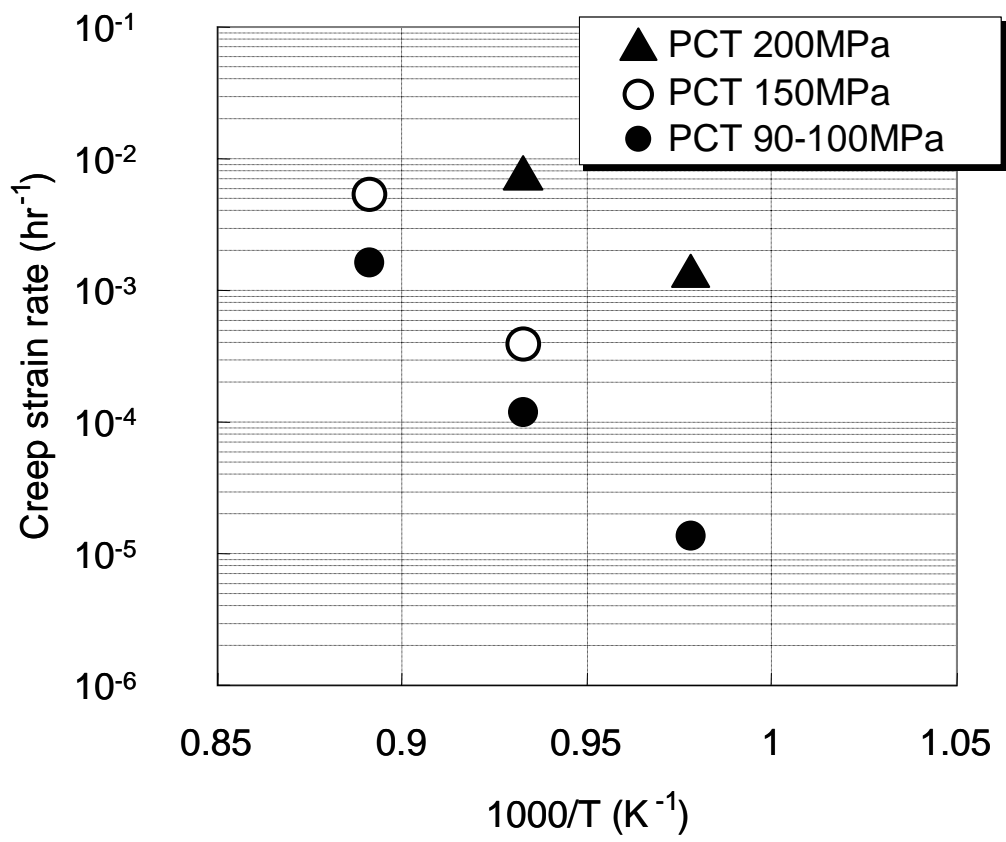


Fig.2. one column

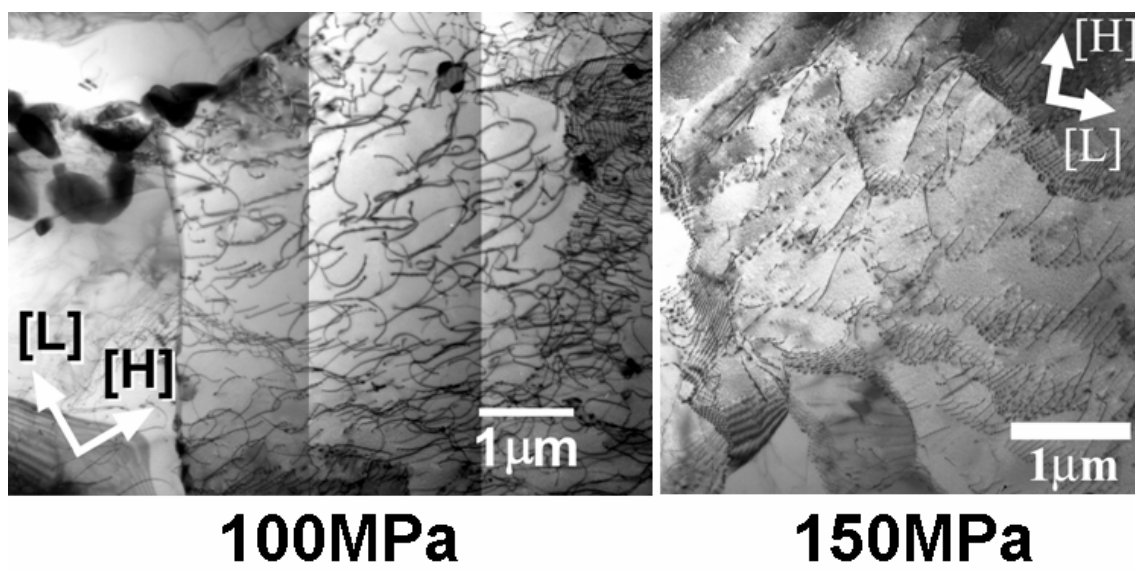


Fig.3. two column

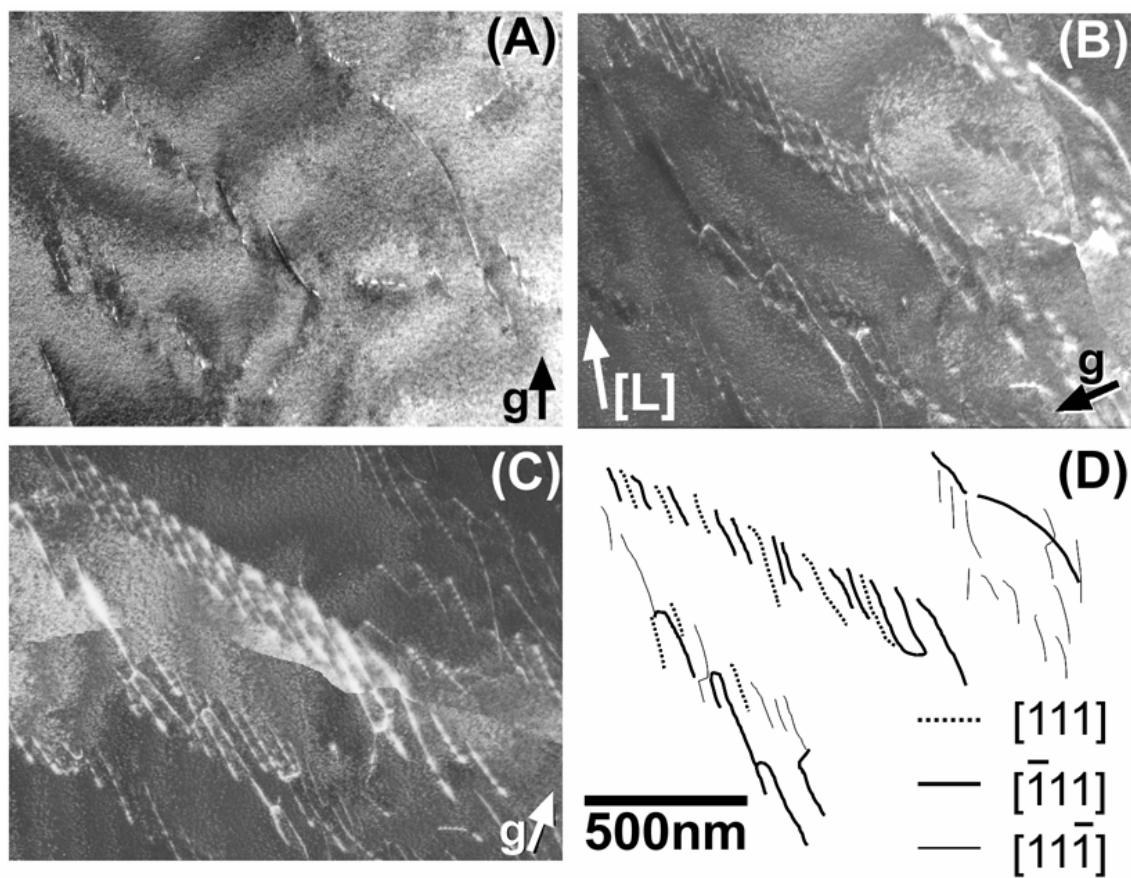


Fig.4. two column

Table 1. : Creep test conditions for NIFS-Heat2 PCTs.

The label (\*) indicates that TEM observations have been performed on that specimen.

Test Temperature ( C)	700	750	800	850
Tubing annealed 2h at 1000C				
	200	200	200	
	150	150	150	150
Effective stress (MPa)	110	100	90	100
			70	
			50	
As-drawn tubing				
Effective stress (MPa)			137	